

## Projectile and Target Z-scaling of Target K-vacancy Production Cross Sections at 10A MeV

R. L. Watson, V. Horvat and K. E. Zaharakis

In two recent studies, attention was focused on the projectile atomic number ( $Z_1$ ) dependence of Al and Cu target atom K-vacancy production cross sections in collision systems for which the ratio of projectile atomic number to target atomic number ( $Z_1/Z_2$ ) ranged from 0.34 to 6.4 [1,2]. It was found that the cross sections for projectiles with  $Z_1 > Z_2$  increase much more slowly as a function of  $Z_1$  than predicted by theoretical (PWBA/ECPSSR) calculations and they appear to approach a saturation limit at high  $Z_1$ . In an attempt to develop a means of estimating K-vacancy production cross sections for heavy ion collisions, a simple scaling law was found that provided a reasonably good representation of the  $Z_1$  dependences of the measured cross sections for both Al and Cu targets [2].

The object of the present work was to examine the general applicability of this scaling law and to investigate further the dependence of heavy ion K-vacancy production cross sections on  $Z_2$ . Using the same 10A MeV beams as in the previous two studies, the investigation has been extended to much higher  $Z_2$  by performing measurements for Mo, Ag, Sn, Sm, and Ta.

The experimental details of the present measurements were nearly identical to those described in Ref. [2]. Thin metallic foils of Mo, Ag, Sn, and Ta, ranging in thickness from 0.79 mg/cm<sup>2</sup> to 2.67 mg/cm<sup>2</sup>, and a Sm target prepared by vacuum evaporating 2.77 mg/cm<sup>2</sup> of metallic Sm onto a thin Al backing were mounted in a target wheel and positioned at a 45° angle relative to both the incident heavy ion beam and a Si(Li) detector. Absolute K<sup>''</sup> x-ray production cross sections were determined for Mo, Ag, and Sn by measuring the K x-ray yields from these targets in

coincidence with particle signals generated by a plastic scintillator detector mounted 4 cm behind the target position. In the cases of Sm and Ta, the cross sections were too small to allow direct particle counting, and so their x-ray yields were measured relative to those observed from Ag monitor foils mounted directly behind the Sm and Ta targets. The Ag monitor absolute x-ray yields per particle were determined in the same way as those for the other targets (i.e., by direct particle counting).

Based on previous target thickness dependence measurements [1,2], the thicknesses of the targets were chosen to give x-ray production cross sections for charge-equilibrated projectiles. Corrections for projectile energy loss have been neglected in this study, but checks performed using the Ag data obtained with the three targets Ag-only, Sm+Al+Ag, and Ag+Ta indicated that corrections to the cross sections for energy loss were less than 5% in the worst case.

Another possible source of error in the present measurements is the neglect of contributions to the K x-ray yields from secondary processes (e.g., photoionization and ionization by secondary electrons). However, based on the  $Z_2$  dependence of x-ray production by secondary processes observed previously for Al and Cu targets [1,2], their contributions are expected to be of the order of 5% for Mo and less than 3% for the rest of the targets.

The measured K<sup>''</sup> x-ray yields per particle were converted to ionization cross sections using normal (single-vacancy) fluorescence yields. Although the fluorescence yields are undoubtedly affected by multiple ionization, the degree of multiple ionization in these relatively high  $Z_2$

targets is thought to be small enough that corrections can be neglected. Moreover, the values of the fluorescence yields are large enough that small changes do not introduce significant errors.

The K-vacancy production cross sections obtained in the present experiments are listed in Table 1, along with the fluorescence yields used to convert them from x-ray production cross sections. Taking into account the errors associated with target thickness, detector efficiency, projectile energy loss, secondary x-ray production, fluorescence yield, and counting statistics, the overall uncertainty in the reported K-vacancy production cross sections is estimated to be  $\pm 12\%$  for Mo, Ag, and Sn, and  $\pm 15\%$  for Sm and Ta.

The K-vacancy production cross sections obtained in this work, together with those obtained previously for Cu [2], are shown in Fig. 1 plotted as a function of  $Z_1$ . The cross sections shown for protons ( $Z_1 = 1$ ) are calculated (ECPSSR) values taken from Ref. [5]. The dashed line in each frame of this figure is drawn at the value of  $Z_1$  that equals the target atomic number ( $Z_2$ ) to delineate the region of symmetric collisions. In the cases of Ag, Sn, Sm, and Ta, it is evident that cross sections near the symmetric collision region

**Table 1:** Cross sections (kb) for K-vacancy production by 10A MeV projectiles and target fluorescence yields ( $H_{K^-}$ ).

Target	$H_{K^-}^a$	Projectile					
		Ne	Ar	Cr	Kr	Xe	Bi
Mo	0.64	8.5(0)	2.5(1)	4.3(1)	4.2(1)	5.7(1)	6.3(1)
Ag	0.68	3.0(0)	8.6(0)	1.2(1)	1.7(1)	3.3(1)	2.4(1)
Sn	0.70	1.8(0)	4.5(0)	5.9(0)	8.3(0)	2.1(1)	1.2(1)
Sm	0.73	2.3(-1)	4.3(-1)	4.5(-1)	6.7(-1)	3.0(0)	2.3(0)
Ta	0.75	4.2(-2)	8.4(-2)	9.5(-2)	1.3(-1)	5.0(1)	1.2(1)

<sup>a</sup> The  $K^-$  fluorescence yield ( $H_{K^-}$ ) is equal to  $H_K(1+R)^{-1}$ , where  $H_K$  is the K-shell fluorescence yield (from Ref. [3]) and  $R$  is the ratio of the  $K^-$  and  $K^+$  x-ray intensities (from Ref. [4]).

(shown by the empty circle data points) are much larger than would be expected from the systematic

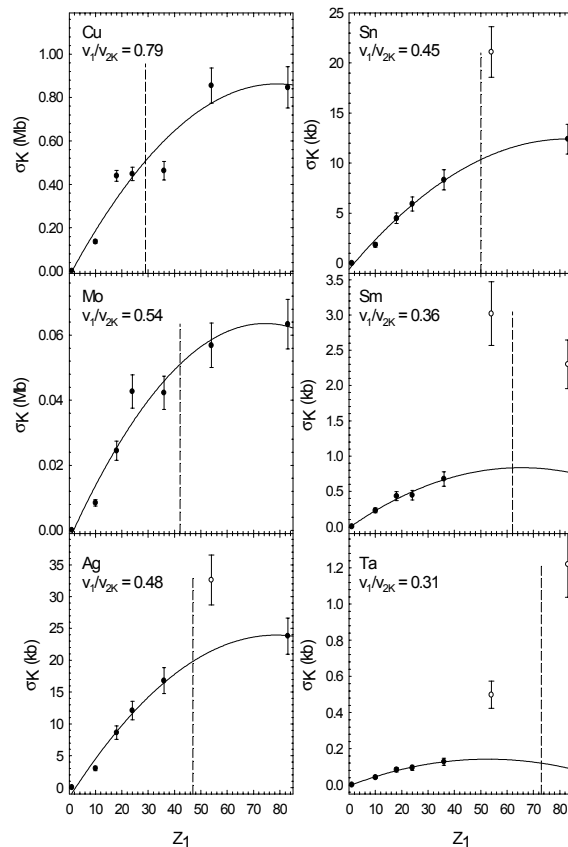


**Figure 1:** K-vacancy production cross sections for the indicated target elements as a function of projectile atomic number. See text for further information.

trend of the cross sections in neighboring asymmetric collision regions (shown by the filled circle data points). Quadratic curves have been fit through the filled circle data points to emphasize this fact. Presumably, the enhanced cross sections for these near symmetric collision systems arise from the well established electron promotion mechanism associated with crossings of quasimolecular orbitals [6]. The cross sections for Cu and Mo do not display a similar enhancement in the region of symmetric collisions. This fact suggests that electron promotion does not contribute in a major way to K-vacancy production cross sections at relative velocities ( $v_1/v_{2K}$ ) above 0.5.

The  $Z_1$ -dependence of the Cu and Al K-vacancy production cross sections determined in the

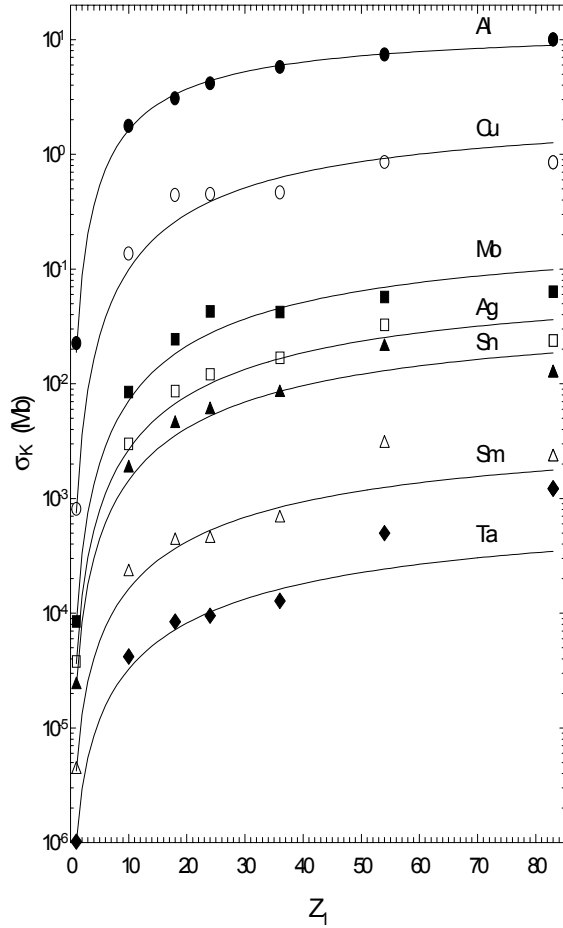


**Figure 2:** Fits of the scaling law to the K-vacancy production cross sections (solid curves).

previous studies [1,2] were reasonably well represented by the empirical scaling law

$$\sigma(Z_1) = \sigma(1) Z_R^m,$$

where  $\sigma(Z_1)$  is the K-vacancy production cross section for projectiles of atomic number  $Z_1$ ,  $\sigma(1)$  is the K-vacancy production cross section for protons,  $Z_R$  is the reduced atomic number defined by

$$Z_R = \frac{Z_1 Z_2}{Z_1 + Z_2},$$

and  $m$  is an exponent that slowly varies with  $Z_2$ . Fits of the above scaling law to the cross sections determined in the present work and to the cross sections for Cu and Al determined previously, are shown by the solid curves in Fig. 2. In making

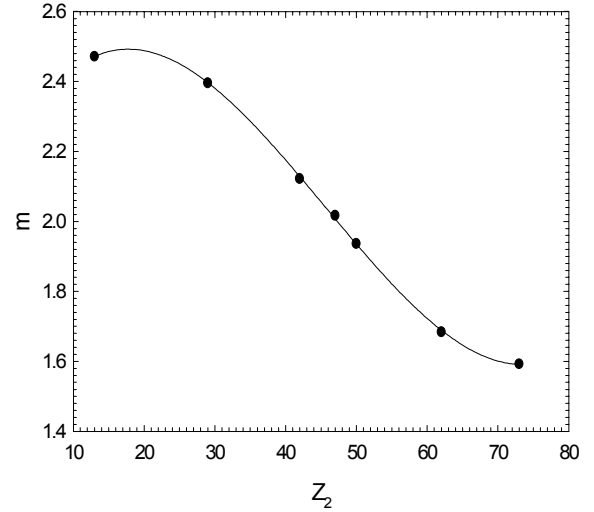


**Figure 3:** Dependence of the scaling law exponent on target atomic number. The curve shows a third order polynomial fit to the data.

these fits, the enhanced cross sections for Ag, Sn, Sm, and Ta (shown by the open circle data points in Fig. 1) were excluded. Overall, the scaling law represents the general trend of most of the data reasonably well (with the exception of the enhanced cross section data points). The dependence of the scaling law exponent  $m$  on  $Z_2$  is shown in Fig. 3. A third order polynomial (solid curve) fits the data very well and provides a means for estimating the exponent at other values of  $Z_2$ . The equation of this fitting function is  $m = 2.158 + 4.091 \times 10^{-2} Z_2 - 1.431 \times 10^{-3} Z_2^2 + 1.046 \times 10^{-5} Z_2^3$ .

### References

- [1] R. L. Watson, J. M. Blackadar, and V. Horvat, Phys. Rev. A **60**, 2959 (1999).
- [2] R. L. Watson, V. Horvat, J. M. Blackadar, and K. E. Zaharakis, Phys. Rev. A **62** (in press).
- [3] A. Langenberg and J. van Eck, J. Phys. **B12**, 1331 (1979).
- [4] J. H. Scofield, Phys. Rev. **9**, 1041 (1974).
- [5] D. D. Cohen and M. Harrigan, At. Data Nucl. Data Tables **33**, 255 (1985).
- [6] R. Anholt, Rev. Mod. Phys. **57**, 995 (1985).